J|A|C|S ARTICLES

Published on Web 11/18/2010

Elucidating the Ionomer-Electrified Metal Interface

Ian Kendrick,[†] Dunesh Kumari,[†] Adam Yakaboski,[†] Nicholas Dimakis,*[,‡] and Eugene S. Smotkin*[,†]

Department of Chemistry and Chemical Biology, Northeastern University, 360 Huntington Avenue, Boston, Massachusetts 02115, United States, and Department of Physics and Geology, University of Texas—Pan American, 1201 West University Drive, Edinburg, Texas 78539, United States

Received September 9, 2010; E-mail: esmotkin@gmail.com; dimakis@utpa.edu

Abstract: The competitive adsorption of Nafion functional groups induce complex potential dependencies (Stark tuning) of vibrational modes of CO adsorbed (CO_{ads}) on the Pt of operating fuel cell electrodes. Operando infrared (IR) spectroscopy, polarization modulated IR spectroscopy (PM-IRRAS) of Pt—Nafion interfaces, and attenuated total reflectance IR spectroscopy of bulk Nafion were correlated by density functional theory (DFT) calculated spectra to elucidate Nafion functional group coadsorption responsible for the Stark tuning of CO_{ads} on high surface area fuel cell electrodes. The DFT calculations and observed spectra suggest that the side-chain CF_3, CF_2 groups (i.e., of the backbone and side chain) and the SO_3^- are ordered by the platinum surface. A model of the Nafion—Pt interface with appropriate dihedral and native bond angles, consistent with experimental and calculated spectra, suggest direct adsorption of the CF_3 and SO_3^- functional groups on Pt. Such adsorption partially orders the Nafion backbone and/or side-chain CF_2 groups relative to the Pt surface. The coadsorption of CF_3 is further supported by Mulliken partial charge calculations: The CF_3 fluorine atoms have the highest average charge among all types of Nafion fluorine atoms and are second only to the sulfonate oxygen atoms.

Introduction

The demand for renewable energy puts fuel cells at the forefront of energy conversion device development.[1−3] Polymer electrolyte membrane fuel cells (PEMFCs) incorporate an ionomer membrane (e.g., Nafion 117) for support of electrocatalytic layers and proton conduction between the electrodes and to maintain separation between the hydrogen and air.[4] A solubilized version of Nafion[5] (ionomer solution) is often used to prepare catalyst "inks" that are directly painted or decal transferred to the membrane.[6] The ionomer—metal interface formed after evaporation of the ink solvent is central to PEMFC electrocatalysis. For example, a spin coated Nafion layer on polycrystalline Pt enhances electrocatalysis.[7,8] Little is known about ionomer—metal interfaces. Markovic and co-workers probed Pt—electrolyte interfaces by measurements of CO oxidation currents, in sulfuric, perchloric, and KOH solutions, synchronized with IR absorption—reflection spectroscopy of linear (ν_{CO}^{l}) and bridge bound (ν_{CO}^{b}) CO_{ads} on Pt(111).[9] More recently their electrochemical studies on Pt(*hkl*)—Nafion interfaces suggest that the Nafion sulfonate group adsorbs onto the Pt surface.[10]

That the active state of a catalyst exists only during catalysis is rationale for operando (actual reactor conditions) characterization of the catalyst—ionomer interface.[11] A fuel cell membrane electrode assembly uniquely enables study of the ionomer metal interface without interferences due to mobile anions characteristic of aqueous acidic electrolytes. Operando fuel cell infrared (IR) spectroscopy was introduced by Fan et al.[12] In this report the aggregate of operando spectroscopy of fuel cell membrane electrode surfaces, attenuated total reflectance spectroscopy of Nafion 117, polarization modulated IR reflection absorption spectroscopy of Nafion spin-coated onto Pt, and density functional theory calculated Nafion spectra suggest a model for the Pt—Nafion interface that includes the Nafion CF_3 group as an important coadsorbate at the ionomer—Pt interface.

Experimental Section

Attenuated Total Reflectance (ATR) Spectroscopy. A surface pressure of 815 psi was maintained over the 1.8 mm diameter ATR crystal. Spectra were obtained using a Bruker Vertex 70 and Vertex 80 V vacuum FTIR spectrometer (Bruker, Billerica, MA). A MIRacle ATR accessory (Pike Technologies Spectroscopic Creativ-

[†] Northeastern University.
[‡] University of Texas-Pan American.

(1) Demirdoven, N.; Deutch, J. *Science* **2004**, *305*, 974.
(2) Diat, O.; Gebel, G. *Nat. Mater.* **2008**, *7*, 13.
(3) Hoogers, G., Ed.; *Fuel Cell Systems Explained*, 2nd ed.; CRC Press LLC: Boca Raton, FL, 2003.
(4) Gottesfeld, S.; Zawodzinski, T. A. *Advances in Electrochemical Science and Engineering*; Wiley-VCH: 1997; Vol. 5.
(5) Martin, C. R.; Rhoades, T. A.; Ferguson, J. A. *Anal. Chem.* **1982**, *54*, 1639.
(6) Wilson, M. S.; Gottesfeld, S. *J. Appl. Electrochem.* **1992**, *22*, 1.
(7) Liu, L.; Viswanathan, R.; Liu, R. X.; Smotkin, E. S. *Electrochem. Solid State Lett.* **1998**, *1*, 123.
(8) Ploense, L.; Salazar, M.; Gurau, B.; Smotkin, E. S. *Solid State Ionics* **2000**, *136−137*, 713.
(9) Stamenkovic, V.; Chou, K. C.; Somorjai, G. A.; Ross, P. N.; Markovic, N. M. *J. Phys. Chem. B* **2005**, *109*, 678.
(10) Subbaraman, R.; Strmcnik, D.; Stamenkovic, V.; Markovic, N. M. *J. Phys. Chem. C* **2010**, *114*, 8414.
(11) Topsoe, H. *J. Catal.* **2003**, *216*, 155.
(12) Fan, Q.; Pu, C.; Lay, K. L.; Smotkin, E. S. *J. Electrochem. Soc.* **1996**, *143*, L21.

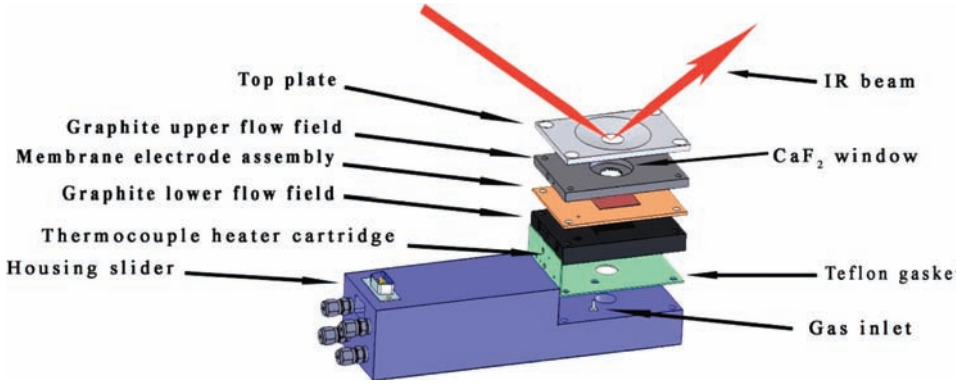

Figure 1. Exploded view schematic of operando spectroscopy cell.

ity, Madison, WI) with a ZnSe ATR crystal was used. The spectra were signal averaged from 100 scans at 4 cm^{-1} resolution with a dry-air purge at ambient temperature. Atmospheric compensation (to eliminate H_2O and CO_2 interference in the beam path) was used in all measurements. Data processing for all infrared data was done with the Bruker OPUS 6.5 software.

Preparation of Arc-Melt Pt. The preparative method for arc-melted electrodes has been described.[13] Briefly, the arc-melter (Materials Research Furnaces, Sun Cook, NH) was charged with 3 mm Pt shot (99.9+%, Sigma-Aldrich, St. Louis, MO). The chamber was evacuated to −29 psig and purged with argon three times. The Pt was arc-melted at 75 A under an Ar bleed. The chamber was vented to flip and arc-melt the sample three times. The Pt slug was epoxied (Devcon HP250, Danvers, MA) to a modified glass syringe barrel, cut flat using a diamond cutoff saw (Buehler IsoMet 1000, Lake Bluff, IL), and finally polished to a mirror finish using 0.05 μm aluminum oxide (Magner Scientific, Dexter, MI). The electrode was sonicated in Nanopure water (Milli-Q, Billerica, MA) for 10 min. Nafion ionomer solution (20 μL) was pipetted onto the Pt electrode assembly mounted on an inverted electrode rotator (Pine Instrument Company, Grove City, Pa) and then rotated (1000 rpm, 1 min).

Polarization Modulated Infrared Reflection Absorption Spectra (PM-IRRAS). The Vertex 80 V spectrometer was equipped with a Hinds II/ZS50 photoelastic modulator (Hinds Instruments, Hillsboro, OR), SR830 lock-in amplifier (Stanford Research Systems, Sunnyvale, CA), and a D3131\6 MCT detector (Infrared Associates, Stuart, FL). The angle of incidence was 60°, and the photoelastic modulator frequency was 50.14 kHz. The PM-IRRAS cell design has been reported.[14,15] Spectra were averaged (710 scans; 4 cm^{-1} resolution). Li-exchanged Nafion was prepared by soaking Nafion samples in 0.1 M salt solutions.

Computational Method. Unrestricted DFT[16,17] with the X3LYP[18] functional was used for geometry optimization and calculations of the normal-mode frequencies and corresponding IR spectra of the deprotonated and protonated Nafion side-chain and backbone segment. The backbone-segment terminal ends were substituted with CH_3 groups to eliminate computational interference with the Nafion CF_3 group. Jaguar 6.5 (Schrodinger Inc., Portland, OR) was used with the all-electron 6-311G**++ Pople triple-ζ basis set ("**" and "++" denote polarization[19] and diffuse[20] basis set functions, respectively). Output files were converted to vibrational mode animations using Maestro (Schrodinger Inc.). Calculations were carried out on a 55 node (dual core Xeon processors with 4GB RAM) High Performance Computing Cluster at the University of Texas, Pan American.

Membrane Electrode Assembly Preparation. Nafion-117 (E. I. DuPont) was immersed in boiling ~8 M nitric acid for 20 min, rinsed with Nanopure water, and finally immersed in boiling water for 1 h. Catalyst inks were prepared as previously described.[21,22] Briefly, Pt black (Johnson Matthey) was dispersed in a 5 wt % Nafion ionomer solution (Sigma Aldrich, Milwaukee, WI) diluted with Nanopure water and isopropyl alcohol. Inks were applied directly to a 5 cm^2 area of Nafion immobilized on a temperature controlled vacuum table (NuVant Systems Inc., Crown Point, IN) at 70 °C. The catalyst loadings were 4 mg/cm^2 of Pt black. The carbon paper gas diffusion layers (Toray Industries, Tokyo, Japan) were blocked with Vulcan XC-72 (Cabot Corporation, Billerica, MA).

Operando Spectroscopy. Temperature dependent CO_{ads} Stark tuning data were acquired by operando specular reflectance IR spectroscopy using a cell (Figure 1) based on the design of Fan et al.[12] The cell, controlled by an EZstat potentiostat (NuVant Systems Inc.), interfaces to a diffuse reflectance accessory (Pike Technologies, Madison, WI) installed on the Vertex 70 spectrometer. The IR beam accesses the working electrode surface through a CaF_2 window inserted into the upper flow field and a small slot in the carbon gas diffusion layer. The lower flow field electrode serves as both a hydrogen reference and counter electrode when charged with hydrogen. The small CO oxidation currents do not measurably polarize the hydrogen counter electrode. The working electrode was cycled (50 times) from 0 to1.2 V vs the hydrogen counter electrode. Spectra were obtained by averaging 250 scans at 4 cm^{-1} resolution. The cell was brought to the desired temperature and potential (300 mV) for the acquisition of reference spectra. Carbon monoxide was passed over the working electrode for 15 min. The cell was purged with N_2 (15 min) prior to setting the potential to 100 mV. Replicates of four spectra were acquired at 50 mV increments until the CO vibrational bands were no longer observable.

Results and Discussion

Operando Spectroscopy. Stark tuning plots of CO_{ads} on Pt in a fuel cell operated at 30, 50, and 70 °C (Figure 2) show a remarkable similarity to plots obtained by Stamenkovic et al. in sulfuric acid.[9] They correlated complex potential dependences (Stark tuning), of CO_{ads} vibrational frequencies (i.e., $d\nu_{CO}^{l}/dE$

(13) Ley, K. L.; Liu, R.; Pu, C.; Fan, Q.; Leyarovska, N.; Segre, C.; Smotkin, E. S. *J. Electrochem. Soc.* **1997**, *144*, 1543.
(14) Kunimatsu, K.; Golden, W. G.; Seki, H.; Philpott, M. R. *Langmuir* **1985**, *1*, 245.
(15) Kunimatsu, K. *J. Electroanal. Chem.* **1986**, *213*, 149.
(16) Hohenberg, P.; Kohn, W. *Phys. Rev. B* **1964**, *136*, B864.
(17) Kohn, W.; Sham, L. J. *Phys. Rev.* **1965**, *140*, 1133.
(18) Xu, X.; Zhang, Q.; Muller, R. P.; Goddard, W. A. *J. Chem. Phys.* **2005**, *122*, 14.
(19) Frisch, M. J.; Pople, J. A.; Binkley, J. S. *J. Chem. Phys.* **1984**, *80*, 3265.
(20) Clark, T.; Chandrasekhar, J.; Spitznagel, G. W.; Schleyer, P. *J. Comput. Chem.* **1983**, *4*, 294.
(21) Gurau, B.; Smotkin, E. *J. Power Sources* **2002**, *112*, 339.
(22) Stoupin, S.; Chung, E.-H.; Chattopadhyay, S.; Segre, C. U.; Smotkin, E. S. *J. Phys. Chem. B* **2006**, *110*, 9932.

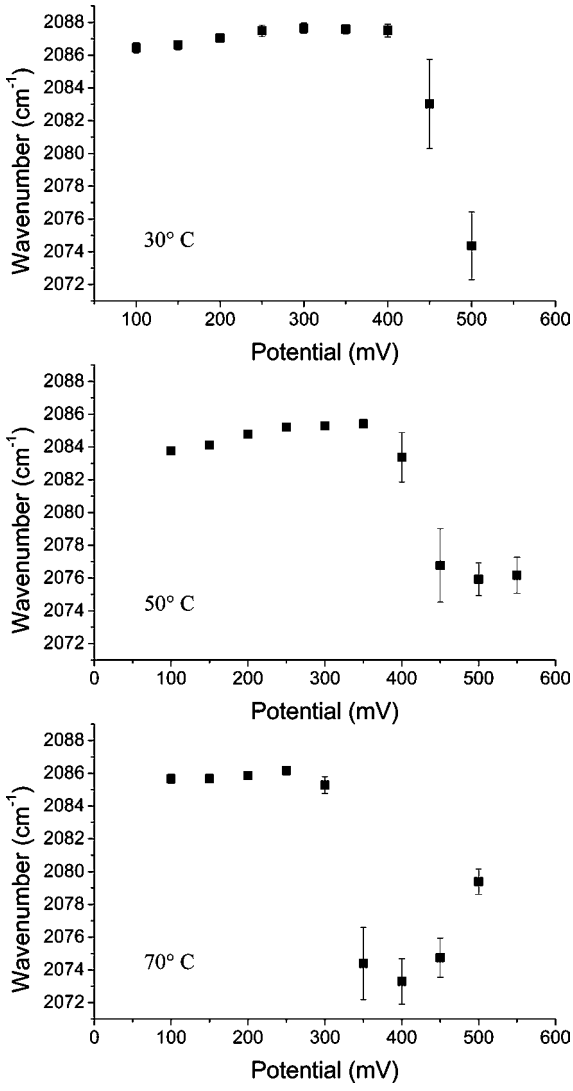

Figure 2. Stark tuning of adsorbed CO on the Pt membrane electrode assembly of an operating fuel cell.

and $d\nu_{CO}^{b}/dE$) in 0.5 M H_2SO_4, to the compression/dissipation of CO_{ads} islands: after a linear region from 0.1 to 0.3 V ($d\nu_{CO}^{l}/dE = 31$ cm^{-1}/V), a subtle ν_{CO}^{l} blue shift from the extrapolated linear region was followed by a precipitous drop, initiating at 0.5 V, that finally upturns at 0.65 V. They attribute this behavior to CO_{ads} island compression due to repulsive dipole interactions with a coadsorbed bisulfate ion initially observable at 0.35 V. CO_{ads} oxidation initiating at 0.5 V, induced by OH^- absorption, diminishes dipole−dipole coupling[23] and thus decreases $d\nu_{CO}^{l}/dE$. The upturn is attributed to an increased absorption of HSO_3^- relative to OH^-, which reestablishes repulsive dipole interactions that compress CO_{ads} islands and increase ν_{CO}^{l}. The plots in Figure 2 demonstrate an adsorption phenomenon onto Pt despite the lack of mobile ions typical of dilute sulfuric acid solutions. The fuel cell operando spectroscopy suggests a need for elucidation of Nafion functional groups responsible for modulation of CO/Pt interactions (i.e., Stark tuning).

Figure 3 shows the linear temperature dependence of the frequency at which the Stark tuning curves precipitously decrease: higher operating temperatures lower the potential at which CO oxidizes (−2.88 cm^{-1}/K, $R^2 = 0.991$). The relationship of this linear variation to the kinetics of the inner sphere processes[24] will be addressed in future work.

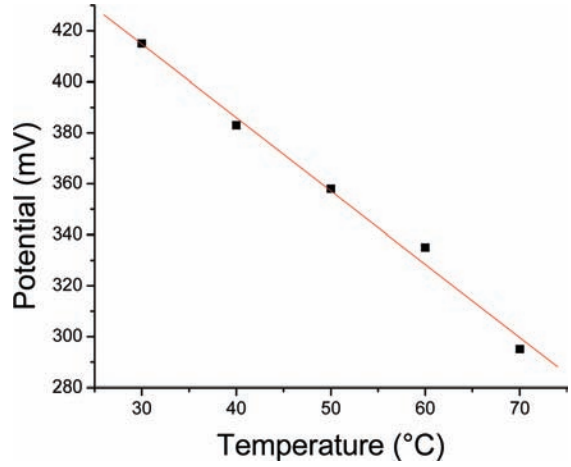

Figure 3. Potential at which CO begins to oxidize as a function of temperature.

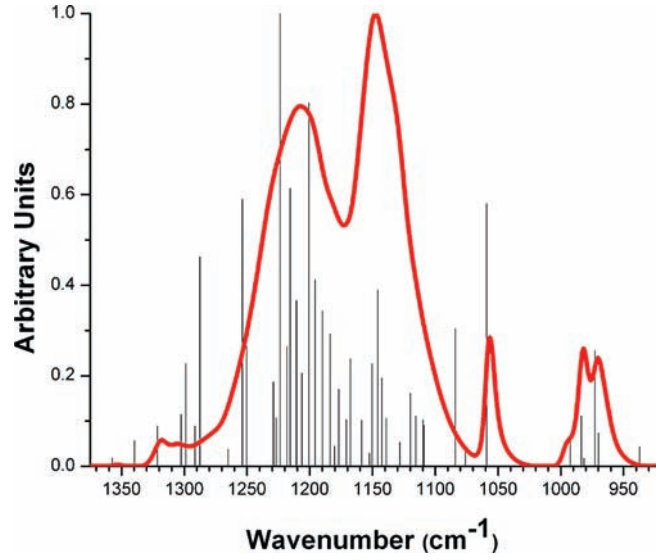

Figure 4. DFT calculated normal modes (black lines) and Nafion ATR spectrum (red).

Analysis of IR Spectra. The DFT calculated spectrum of a 55-atom Nafion side-chain and backbone segment provides 159 normal-mode frequencies and intensities. Figure 4 shows the theoretically derived peak positions and intensities (black lines) superimposed upon the ATR spectrum (red line) of hydrated Nafion.

PM-IRRAS enhances (relative to the ATR) vibrational modes of functional groups ordered by the Pt surface. Figure 5 shows the ATR spectrum (red), the PM-IRRAS spectra of the Nafion-H/Pt interface (gray line) and the Nafion-Li/Pt interface of Li^+ exchanged Nafion (blue line), and six selected (from the 159 calculated) DFT calculated frequencies and intensities.

Scheme 1 is the Nafion structure with functional groups labeled for ease of discussion. The low-frequency ATR band (Figure 5) at 971 cm^{-1} (corresponding to theoretical 984 cm^{-1}; line 1) and the 1056 cm^{-1} band (corresponding to theoretical 1059 cm^{-1}; line 3) have recently been thoroughly assigned by

(23) Persson, B. N. J.; Ryberg, R. *Phys. Rev. B* **1981**, *24*, 6954.

(24) Bard, A. J. *J. Am. Chem. Soc.* **2010**, *132*, 7559.

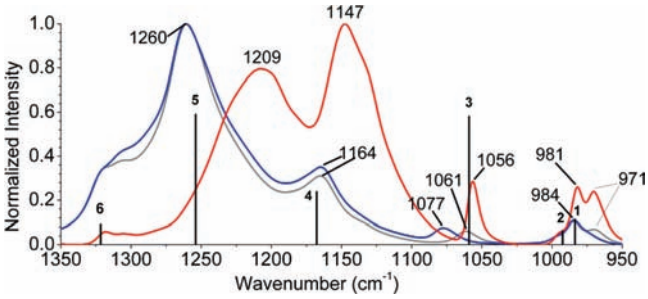

Figure 5. Theoretical and experimental spectra. ATR of hydrated Nafion (red); PM-IRRAS of Nafion-H on Pt (gray); PM-IRRAS of Nafion-Li on Pt (blue); Selected DFT peaks (black lines 1−6).

Scheme 1. Segment and Atom Labeling for Nafion

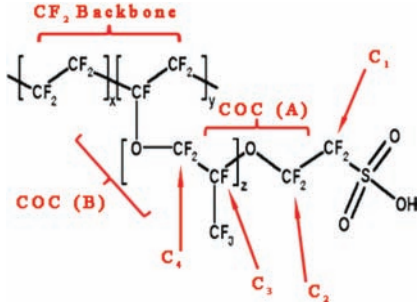

Webber et al.[25] They obtained high resolution transmission spectra of hydrated and thoroughly dehydrated Nafion and analyzed them in the context of the spectroscopy of the short chain ionomer (formerly DOW membrane), the Nafion sulfonyl fluoride,[26] and the Nafion sulfonyl imide.[27] Animations of the DFT calculated internal coordinates reveal that the observed 1056 and 971 cm^{-1} peaks both have internal coordinates resulting from the mechanical coupling of the adjacent sulfonate and COC (A) ether link.[25] Thus these peaks shift concertedly with changes in the sulfonate environment. Consider the ATR and PM-IRRAS spectra of the protonic form of Nafion (Figure 5, gray line). The 1056 and 971 cm^{-1} peaks concertedly shift to higher frequencies in the PM-IRRAS because of the interaction of the sulfonate functional group with the Pt surface. A similar effect is observed with Li^+ exchange of the adsorbed Nafion (blue line).

A convention for correlating PM-IRRAS enhanced peaks to the calculated DFT peaks would enable identification of functional groups ordered by the Pt surface: The association of observed PM-IRRAS peaks with DFT peaks, assigned by visualization of mechanically coupled internal coordinates,[25,28] provides the basis for such a convention. Normal mode coordinate animations (generated by Maestro from DFT output files) explicitly show how neighbor functional groups (called out in Scheme 1) are mechanically coupled. The calculated internal coordinates are viewed in the context of calculated normal modes of relevant small molecules (e.g., triflic acid, CF_3OCF_3, 10-carbon CF_2 backbone, etc.) hereafter referred to as "pure modes," which serve as the basis elements for assigning DFT calculated normal modes associated with observed peaks. Figure 6 shows the assignments of the six selected DFT peaks and snapshots of the corresponding Maestro animations. The atoms contributing to the dominating motion (black circles) and the next most significant atom motions (dotted circles) comprise pure modes that form the basis for the assignments. An alternate strategy for determining the dominant mode is to consider the contribution to the potential energy surface on an atom by atom basis.[29] While this may change the selection of the dominant mode, it does not alter what pure modes contribute to the assignments. The correlation of the DFT to PM-IRRAS peaks (Figure 5) and the resulting assignments in terms of the mechanically coupled modes are tabulated in Table 1.

The pure mode peak assignments (Table 1) elucidate functional groups ordered by the Pt surface. Animations of the pure modes and the internal coordinates of the six selected peaks are in Movies 1−12 and Movies 13−18 respectively in the Supporting Information as.AVI files. The rationale for the key functional group assignments (Table 1) is supported by the overlap of the DFT calculated peak positions with the PM-IRRAS peaks. Consider the DFT and PM-IRRAS peaks in the context of the bulk-Nafion ATR and the report by Cable et al.[26] that the 1056 and 971 cm^{-1} peaks shift with alterations of the sulfonate group environment. The bulk ATR peak at 1056 cm^{-1} (red), the PM-IRRAS peak of protonated Nafion adsorbed on Pt (gray line) at 1061 cm^{-1}, and the PM-IRRAS peak of lithiated Nafion adsorbed on Pt (blue line) at 1077 cm^{-1} (Figure 5) confirm that Pt surface atoms induce frequency *shifts*, as do the extent-of-hydration[25] and ion exchange of Nafion.[26] Thus the PM-IRRAS enhances bulk-Nafion modes that are shifted due to functional group interactions with Pt. Less explicit than the 1056 cm^{-1} peak are PM-IRRAS peaks derived from bulk-Nafion modes that are convoluted within the Nafion ATR broad envelope region (1100−1300 cm^{-1}), in particular the 1164 and 1260 cm^{-1} PM-IRRAS peaks. Di Noto et al.[30] extensively deconvoluted the broad envelope region. Their resulting peak library includes 1148, 1245 cm^{-1}, which could be reconciled with an association of the DFT peaks (Figure 5, lines 4 and 5) with the *shifted* PM-IRRAS peaks at 1164 and 1260 cm^{-1}.

Nafion/Pt Adsorption Model. The animation of the theoretical peak at 1254 cm^{-1} (Figure 5, line-5), associated with PM-IRRAS peaks at 1260 cm^{-1} (blue and gray lines), suggests that the CF_3 internal coordinates dominate the normal mode. The insensitivity of the 1201 cm^{-1} peak, to ion exchange, suggests that the internal coordinates are not substantially coupled to the sulfonate group. The 1260 cm^{-1} band intensity is over an order of magnitude greater than that of the cluster of peaks (i.e., associated with theoretical lines 1 and 2) that are mechanically coupled to the sulfonate pure mode: The CF_3 functional group is a coadsorbate of comparable importance to the sulfonate exchange group in the formation of the Nafion/Pt interface. Further support for this model is provided by Mulliken population[31] analysis. Atomic charges of the 55 Nafion fragment atoms were calculated. Table 2 shows the average charges of the backbone, side chain, and CF_3 group fluorine atoms and the average charges on the sulfonate oxygen atoms. The charges for chemically equivalent atoms (e.g., CF_3 fluorine and sulfonate oxygen atoms) differ because the calculations are done for the

(25) Webber, M.; Dimakis, N.; Kumari, D.; Fuccillo, M.; Smotkin, E. S. *Macromolecules* **2010**, *43*, 5500.
(26) Cable, K. M.; Mauritz, K. A.; Moore, R. B. *J. Polym. Sci., Part B: Polym. Phys.* **1995**, *33*, 1065.
(27) Byun, C. K.; Sharif, I.; DesMarteau, D. D.; Creager, S. E.; Korzeniewski, C. *J. Phys. Chem. B* **2009**, *113*, 6299.
(28) Warren, D. S.; McQuillan, A. J. *J. Phys. Chem. B* **2008**, *112*, 10535.
(29) Johansson, P. Chalmers University of Technology. *Personal Communication*, 2010.
(30) Di Noto, V.; Piga, M.; Lavina, S.; Negro, E.; Yoshida, K.; Ito, R.; Furukawa, T. *Electrochim. Acta* **2010**, *55*, 1431.
(31) Mulliken, R. S. *J. Chem. Phys.* **1955**, *23*, 1833.

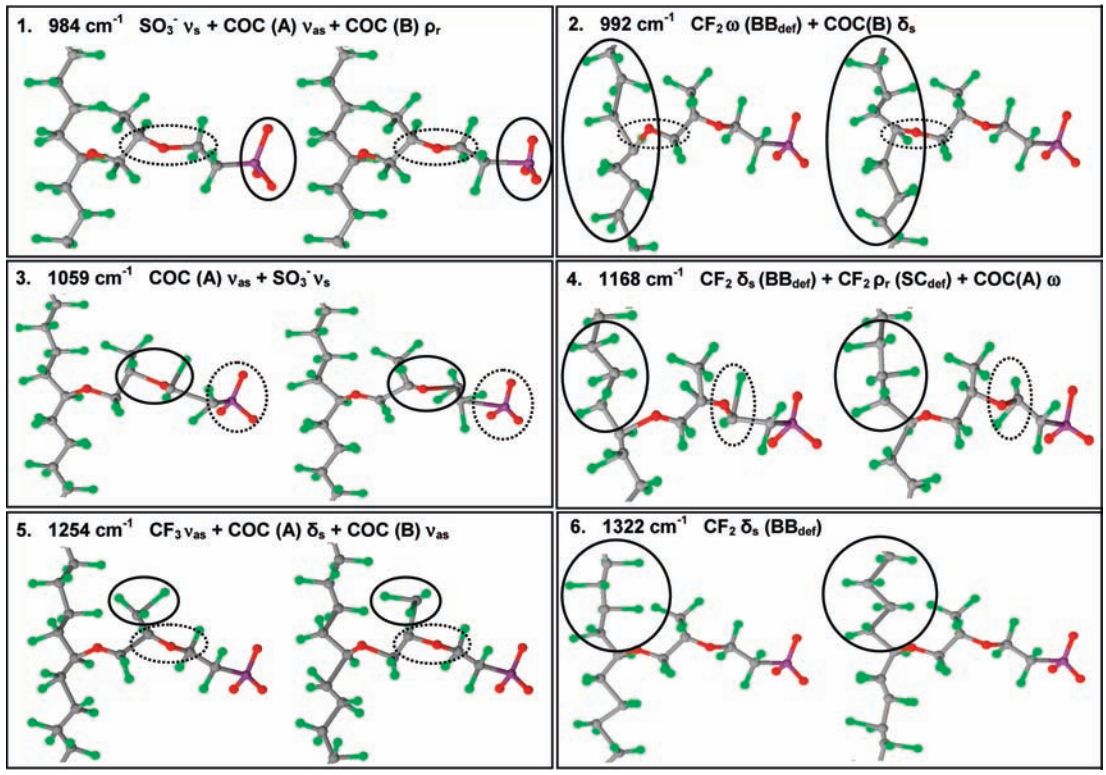

Figure 6. Normal mode coordinate animation snapshots of the Nafion side-chain anion and backbone fragment (see Scheme 1). Left and right views are extrema positions of the vibrational mode. Functional groups associated with the dominant internal coordinates and next most significant motions are designated by solid and dotted boundary lines respectively.

Table 1. PM-IRRAS and DFT IR Adsorption Peaks and Assignments[a]

	Wavenumber (cm^{-1})		
	PM-IRRAS	DFT	Pure Mode Components
1	971	984	SO_3^- $\boldsymbol{\nu}_s$ + COC(A) $\boldsymbol{\nu}_{as}$ + COC(B) $\boldsymbol{\rho}_r$
2	984	992	CF_2 $\boldsymbol{\omega}$ **(BB$_{def}$)** + COC(B) $\boldsymbol{\delta}_s$
3	1061	1059	COC(A) $\boldsymbol{\nu}_{as}$ + SO_3^- $\boldsymbol{\nu}_s$
4	1164	1168	CF_2 $\boldsymbol{\delta}_s$ **(BB$_{stre}$)** + CF_2 **(BB$_{def}$)** $\boldsymbol{\rho}_r$ + COC(A) $\boldsymbol{\omega}$
5	1260	1254	CF_3 $\boldsymbol{\nu}_{as}$ + COC(A) $\boldsymbol{\delta}_s$ + COC(B) $\boldsymbol{\delta}_s$
6	1322	1322	CF_2 $\boldsymbol{\delta}_s$ **(BB$_{def}$)**

[a] Symmetric stretch, ν_s; Asymmetric stretch, ν_{as}; Wagging, ω; Scissoring, δ_s; Twisting, τ; Rocking, ρ_r; Backbone deformation, BB_{def}; Side-chain deformation, SC_{def}; Backbone Stretching, BB_{stre}.

Table 2. Average Partial Charges of Selected Nafion Segments

	Backbone (F)	Side chain (F)	CF_3 (F)	Sulfonate (O)
Segment	13 atoms	8 atoms	3 atoms	3 atoms
Avg Partial Charge	−0.0665	−0.0816	−0.0876	−0.4879
Standard Deviation	0.027	0.055	0.013	0.012

lowest energy Newman projections where the atomic environments are different for chemically equivalent atoms because of the absence of symmetry in the full molecule. The chemically equivalent atoms have smaller charge standard deviations as would be expected. The average charge of the CF_3 fluorine atoms are the highest among the three classes of fluorine atoms (Table 2) and are about 18% that of the sulfonate oxygens.

A Gaussian 03 Viewer (Gaussian, Wallingford, CT) used to construct a 2-equiv (1100 g/equiv) model of Nafion 117 enables rotation of dihedral angles while maintaining the native bond angles associated with each and every functional group. The CF_3 and SO_3^- groups, oriented with the two planes defined by the CF_3 fluorine and sulfonate oxygen atoms parallel to a Pt surface, effect ordering of the CF_2 backbone segments with respect to the Pt surface. Ordering of the CF_2 groups would be expected to yield PM-IRRAS peaks. The PM-IRRAS peak at 1164 cm^{-1} is associated with the theoretical peak (line-4) at 1168 cm^{-1}. The line 4 animation shows that CF_2 backbone internal coordinates dominate the 1168 cm^{-1} mode, supporting the suggestion of ordered CF_2 groups. Figure 7 is the Gaussian View model resulting from orienting the CF_3 and SO_3^- groups for adsorption to the Pt surface. The numbers (yellow) associate DFT calculated IR peaks (lines 1−6, Figure 5) and associated PM-IRRAS peaks with regions of order induced by the CF_3 and SO_3^- functional group adsorbates.

The ordering of the backbone CF_2 groups in the Gaussain model is a natural consequence of adjusting the dihedral angles of the anchoring groups for adsorption, while maintaining functional group native bond angles. Thus the aggregate of the Stark tuning data of Figure 2, the PM-IRRAS, and DFT calculations support Figure 7 as a model for Nafion functional group adsorption to Pt. The details of exactly how adsorbed CF_3 functional groups influence the operando Stark tuning curves is not yet established. The low density of functional group adsorption sites, relative to the number of backbone CF_2 groups, suggests an explanation as to why Nafion is observed to enhance electrode processes.[7,32] The methodology of assigning IR bands in the context of mechanically coupled internal coordinates of neighboring functional groups, and correlating those assignments

(32) Ploense, L.; Salazar, M.; Gurau, B.; Smotkin, E. S. *J. Am. Chem. Soc.* **1997**, *119*, 11550.

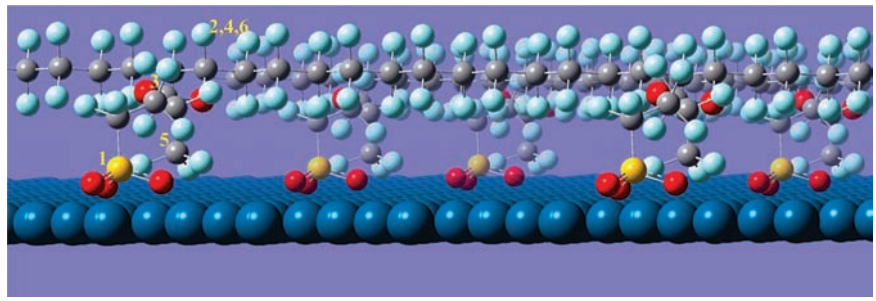

Figure 7. Gaussian 03 Viewer Nafion−Pt interface model. Oxygen (red), Sulfur (yellow), Fluorine (light blue), Carbon (gray), Pt (dark blue).

to functional groups interactions with metal surfaces, has broad applications toward characterization of ionomeric interfaces.

Conclusion

Operando IR spectroscopy, PM-IRRAS of Nafion−Pt interfaces, and ATR spectroscopy of Nafion, correlated with DFT calculated normal-mode frequencies, confirm that Nafion side-chain sulfonate *and* CF_3 coadsorbates are structural components of the Nafion−Pt interface. These "anchoring" functional groups reduce the degrees of freedom available for backbone and side-chain CF_2 dynamics. The partial ordering of Nafion CF_2 groups is supported by observed PM-IRRAS and DFT calculated peaks possessing vibrational internal coordinates dominated by, and mechanically coupled to, side-chain CF_2 group motions.

Acknowledgment. We thank the UT Pan American High Performance Computing Center. This work was funded by the Army Research Office and NuVant Systems Inc.

Supporting Information Available: AVI files of normal mode transitions (AVI file captions in PDF file). This material is available free of charge via the Internet at http://pubs.acs.org.

JA1081487